REPORT DOCUMENTATION PAGE

Form Approved
OMB No. 0704-0188

1. REPORT DATE *(DD-MM-YYYY)*	2. REPORT TYPE	3. DATES COVERED *(From - To)*
29-02-2008	Final Performance Report	Jul 2005 - Nov 2007

4. TITLE AND SUBTITLE

Ferroelastic Plasma Thruster

5a. CONTRACT NUMBER
FA9550-05-1-0421

5b. GRANT NUMBER

5c. PROGRAM ELEMENT NUMBER

6. AUTHOR(S)
Kovaleski, Scott D.
Kemp, Mark A.

5d. PROJECT NUMBER

5e. TASK NUMBER

5f. WORK UNIT NUMBER

7. PERFORMING ORGANIZATION NAME(S) AND ADDRESS(ES)

University of Missouri System
Curators of the University of
Missouri
315 University Hall
Columbia, MO 65211-1302

8. PERFORMING ORGANIZATION REPORT NUMBER

9. SPONSORING / MONITORING AGENCY NAME(S) AND ADDRESS(ES)

USAF, AFRL
AF Office of Scientific Res
875 N. Randolph St., RM 3112
Arlington, VA 22203
Dr Mitat Birkan/NA

10. SPONSOR/MONITOR'S ACRONYM(S)

11. SPONSOR/MONITOR'S REPORT NUMBER(S)

AFRL-SR-AR-TR-08-0069

12. DISTRIBUTION / AVAILABILITY STATEMENT

Approved for public release,
distribution unlimited

13. SUPPLEMENTARY NOTES

14. ABSTRACT

The Ferroelectric Plasma Thruster (FEPT) has been developed as an electrostatic micropropulsion thruster for the smallest classes of spacecraft. The FEPT consists of a thin wafer of lithium niobate ferroelectric material, with a solid electrode on one side, and an electrode with an aperture on the other. When radiofrequency high voltage is applied between the electrodes, through the thickness of the crystal, a combination of triple point and piezoelectric effects produce dense plasma on the crystal surface. The ions from this plasma are accelerated by the applied field on the positive half cycle producing thrusts measured to be between 61 and 87 microNewtons, depending on applied voltage. Electrons are emitted during the negative half cycle, making the device potentially self-neutralizing. The ion beam consisted of silver ions applied to the crystal surface and crystal materials. Ion energies were measured to be about 97 eV with 12 nC in each ion pulse. The specific impulse was measured to be between 183-587 s, with some neutral flow. Thrust efficiency was between 1-4%, with power input between 4 and 20 W.

15. SUBJECT TERMS

electric propulsion, micropropulsion, ferroelectric plasma source

16. SECURITY CLASSIFICATION OF:			17. LIMITATION OF ABSTRACT	18. NUMBER OF PAGES	19a. NAME OF RESPONSIBLE PERSON
a. REPORT	b. ABSTRACT	c. THIS PAGE			19b. TELEPHONE NUMBER *(include area code)*

Ferroelectric Plasma Thruster
Final Performance Report

Award No. FA9550-05-1-0421
Principle Investigator: Dr. Scott Kovaleski
Electrical and Computer Engineering
University of Missouri-Columbia

Program Manager: Dr. Mitat Birkan, AFOSR

1) Introduction/Experimental Setup

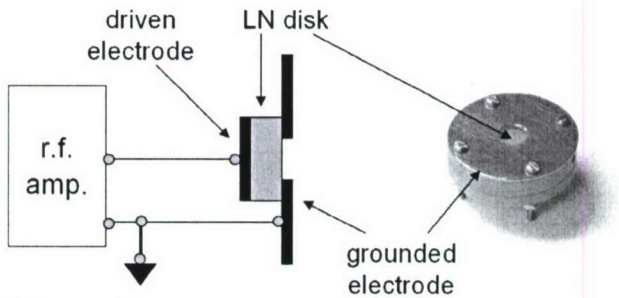

Fig. 1: FEPT diagram and photograph.

For the FEPT, ion emission is the mass transfer mechanism for thrust production. An rf voltage is applied across a ferroelectric disk and a plasma is formed on the ferroelectric surface in a grounded aperture. This plasma serves as a source of ions for subsequent acceleration. The applied rf field electrostatically accelerates ions out of the plasma. When a positive voltage is on the rear of the ferroelectric, ions are repelled from the front ferroelectric surface and eventually exit the device. An electrostatic field simulation, shown in Fig. 2, illustrates the electric field lines with a positive 1 kV voltage applied to the rear electrode. Similarly, electrons are repelled on the negative half-cycle. Repetitive rf cycles result in bursts of ions accelerated away from the FEPT. It has been shown that the plasma forms and dissipates within one rf cycle, within 500-1000 ns typically [Kemp, JAP-2006]. Therefore, the FEPT is a burst thruster, rather than a continuous-on device.

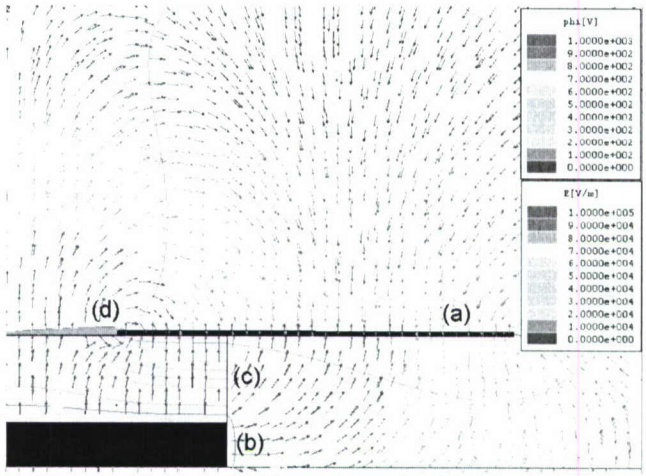

Fig. 2: Electrostatic field simulation. (a) Grounded front electrode, (b) driven rear electrode, (c) ferroelectric, (d) plasma.

2) Plasma Plume Measurements

Initially, open shutter photographs of plasma luminosity were used to confirm plasma formation. Three typical time-integrated photographs are shown in Fig. 3. As shown by fast-framing photographs in the next section, the plasma formed during a single RF cycle is a single filament that forms and extinguishes during every half cycle. The photographs in Fig. 3 show many separate filaments over the majority of the ferroelectric. It is beneficial that the plasma forms at multiple locations from cycle to cycle because any erosion is distributed around the front electrode circumference. This will contribute to increased thruster lifetime.

Fig. 3: Open-shutter photographs of plasma formation in FEPT aperture.

To measure the ion current out of the thruster, a Faraday cup was placed 3 cm in front of the output aperture. Electrostatic simulations were performed to ensure that at this distance, the Faraday cup did not significantly affect the electric field profile due to the driven FEPT electrode, with the penalty that only part of the beam is captured. Also, measured ion current pulses are broadened because of varying times-of-flight from the FEPT to the Faraday cup. Assuming isotropic beam dispersion and correcting for the open area fraction of two grids, Figure 4 shows one measurement of ion current. Typical average charge per pulse is ~12 nC. With a driving frequency of 378 kHz, this yields an average current of ~4.5 mA. A correction factor was used to account for beam dispersion and the grid open area fraction. There is a phase shift between the measured ion beam waveform and the beam waveform at the FEPT exit due to the ion time-of-flight to the Faraday cup.

A retarding potential analyzer was used with a Faraday cup to measure the ion energy

spectrum. In order, from the thruster, there was a grounded grid, a 0-400 V positively biased grid, and a negative 1 kV grid to suppress any electrons from the beam and for Faraday cup secondary electron emission suppression. Electrons with energies close to the same potential as the driving voltage were measured. Also, electrons were measured co-moving with the ion beam which suggests that the beam from FEPT may be neutral. We found that varying the distance of the Faraday cup from the FEPT surface from 1 cm to 15 cm did not significantly alter the measured spectrum.

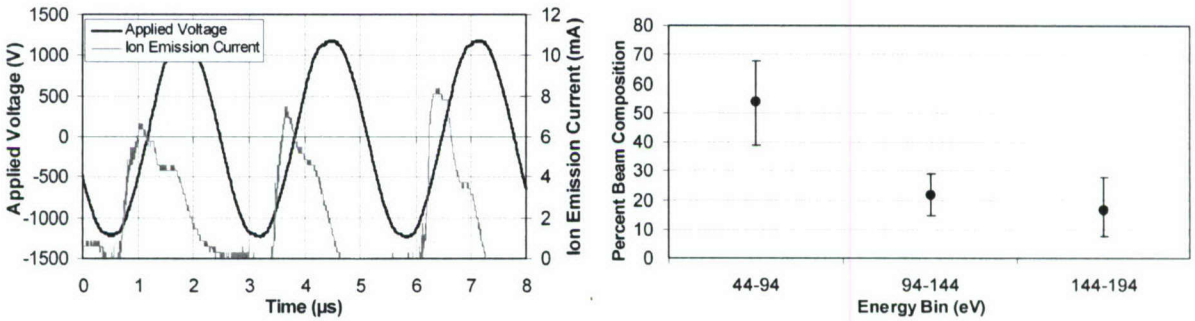

Fig. 4: Left: Measured ion current and driving voltage. Right: Measured ion energy spectrum. Measured ion current with energy less than 44 eV was insignificant. Average ion energy was ~97eV

An Ametek/Dycor M200M gas analyzer quadrupole was used to find the mass of the ions emitted from the FEPT. With the integral ionization filament and acceleration grid turned off, the FEPT with SLN was directed towards the quadrupole input aperture. Ions resolved were the two isotopes of silver, ^{107}Ag and ^{109}Ag, ^{93}Nb, ^{7}Li, as well as doubly ionized Nb. For emission spectroscopy experiments, we used an Acton SpectraPro 2300i 0.3 m spectrograph with gratings of 2400 and 300 grooves/mm. The photocathode of a PI-MAX ICCD camera imaged the output slit of the spectrograph. Among others, the Ag I, Nb I, Li I and Nb II lines were visible. Table II is a summary of some of the mass and emission spectroscopy lines observed. Both the mass and emission spectroscopy experiments are consistent with the proposed theory that a main component of the plasma formed in ferroelectric plasma sources is the ferroelectric itself and electrode materials.

Table I: Summary of measured emission and mass spectroscopy lines.

	Ion	Mass/ionization state (amu)
Mass Spectroscopy	Ag^{+}	108.9,106.9
	Nb^{+}	92.9
	Nb^{++}	46.5
	Li^{+}	6.9
	Spectrum	Wavelengths (nm)
Emission Spectroscopy	Ag I	328.1, 338.3
	Nb I	405.9, 408.0, 410.1, 590.1
	Li I	610.4, 670.8
	Nb II	202.9, 203.3, 210.9

3) Effect of Piezoelectricity

We found correspondence of the radial piezoelectric vibration resonance in the ferroelectric crystal to breakdown voltage in the FPS. Breakdown voltage is defined as the lowest voltage in which there was measured photon emission for every half-cycle of the applied voltage burst (typically ~15 cycles). The breakdown voltages measured for a 1 mm thick PZT disk in atmospheric pressure air are shown in Fig. 5. As the FPS impedance decreases toward the piezoelectric resonance at ~235 kHz, the breakdown voltage decreases to a minimum at the same frequency. The breakdown voltage increases after the frequency is increased above the resonance. Above ~245 kHz, the breakdown voltage was above the maximum output of our driving circuitry. Plasma was not formed with >540 V applied at 255 kHz or with >800 V applied at 270 kHz.

This piezoelectric effect extends to operation in a vacuum background as well. Figure 5 shows breakdown voltages with respect to driving frequency for FPS operation in atmosphere and vacuum backgrounds. At 200 kHz, the breakdown voltage was ~60% and ~50% higher than the atmospheric pressure breakdown voltage for the 1.0 and 0.5 mm thick disks, respectively. However, the difference between the atmospheric pressure and vacuum threshold voltages becomes almost zero at driving frequencies close to the radial resonance. Also shown in Fig. 5 is the effect of disk thickness on the breakdown voltage. Again, at 200 kHz, the breakdown voltage for the 1.0 mm thick disk is higher than the 0.5 mm disk at both vacuum and atmospheric pressure. At the resonant frequency there is no discernable difference.

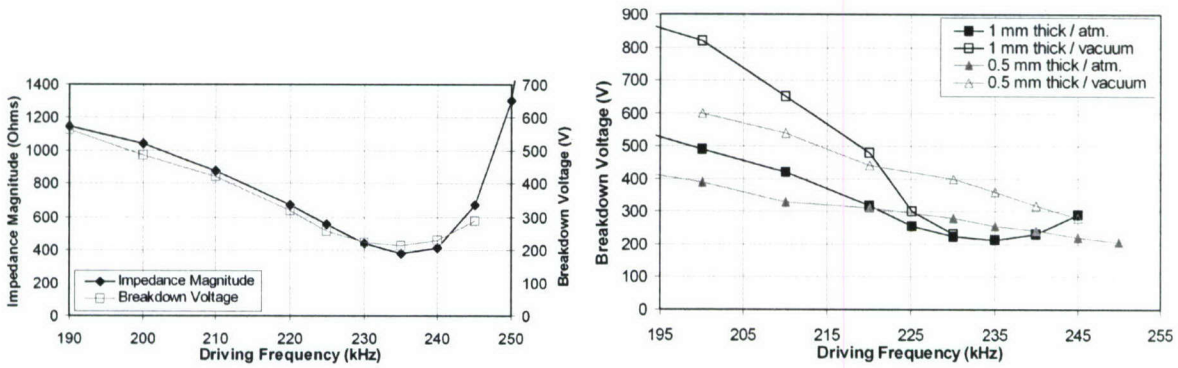

Fig. 5: Left: Measured FEPT impedance and breakdown voltage w.r.t. driving frequency in a background of atmospheric-pressure air. Right: Breakdown voltage for different background pressures and disk thicknesses.

Figure 6 shows simulations of the equipotential lines far below, below, and at the resonance frequency. Far below resonance where piezoelectric effects likely have little effect, the value of the largest equipotential in the aperture is not significantly larger than the applied potential. As the applied frequency is closer to resonance, the value of the maximum potential increases.

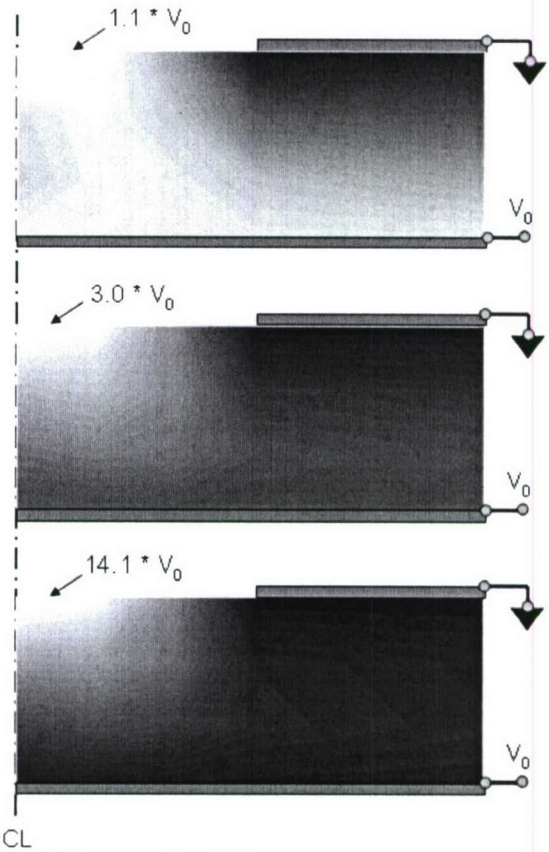

Fig. 6: Finite element simulation of the FEPT for different driving frequencies. From top to bottom: far below resonance, near resonance, and at resonance.

4) Atmospheric-Pressure Operation

The relative intensity of five Ag I lines were used to construct the Boltzmann plot shown in Fig. 7. Using linear regression, the negative inverse slope of the best fit line through data points was 2.3 eV with a 95% confidence interval of 1.8-3.3 eV. The N_2 rotational temperature was found by modeling the 337.13 nm nitrogen band shown in Fig. 7.

Using a front electrode with a 2.9 mm wide channel, Schlieren photographs were taken of the ceramic surface. Shadows appeared in the photograph starting on the ferroelectric surface and expanding away over time. We speculate that this was hot or warm gasses and plasma flowing away from the surface. The calculated velocity is ~4 m/s.

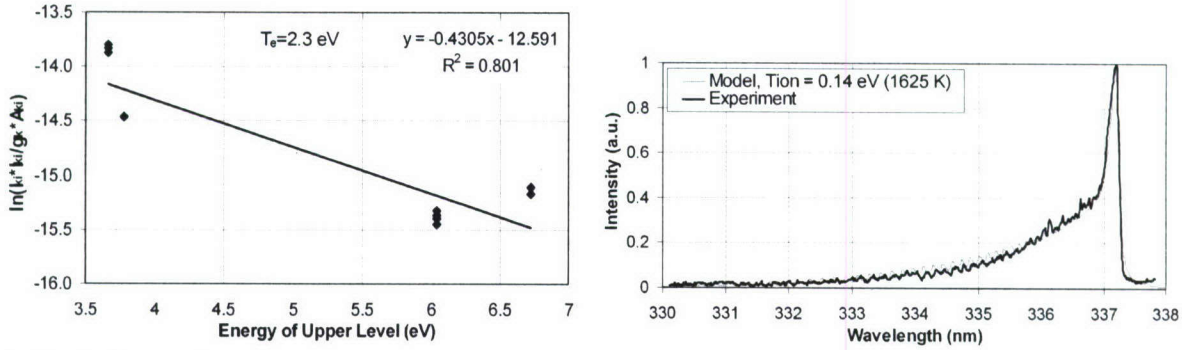

Fig. 7: Left: Atomic-Boltzmann plot of neutral silver lines with the FEPT operating in a background of atmospheric-pressure air. The free-electron temperature was 2.3 eV. Right: Modeled and measured N_2 second-positive band. Modeled rotational temperature is 0.14 eV.

5) Microthruster Characteristics

To directly measure the FEPT thrust, we developed a pulsed thrust stand. The thruster volume and mass are relatively small and only two wires from the power supply located outside the chamber to the thruster were required. Therefore, we were able to mount the thruster, a swinging arm, and a Michelson interferometer all on one 6"x4" optical breadboard. The thrust stand schematic and a photograph are shown in Fig. 8. The HeNe laser, diode detector, and beam expander were located outside the chamber while the rest of the thrust stand was mounted on the breadboard.

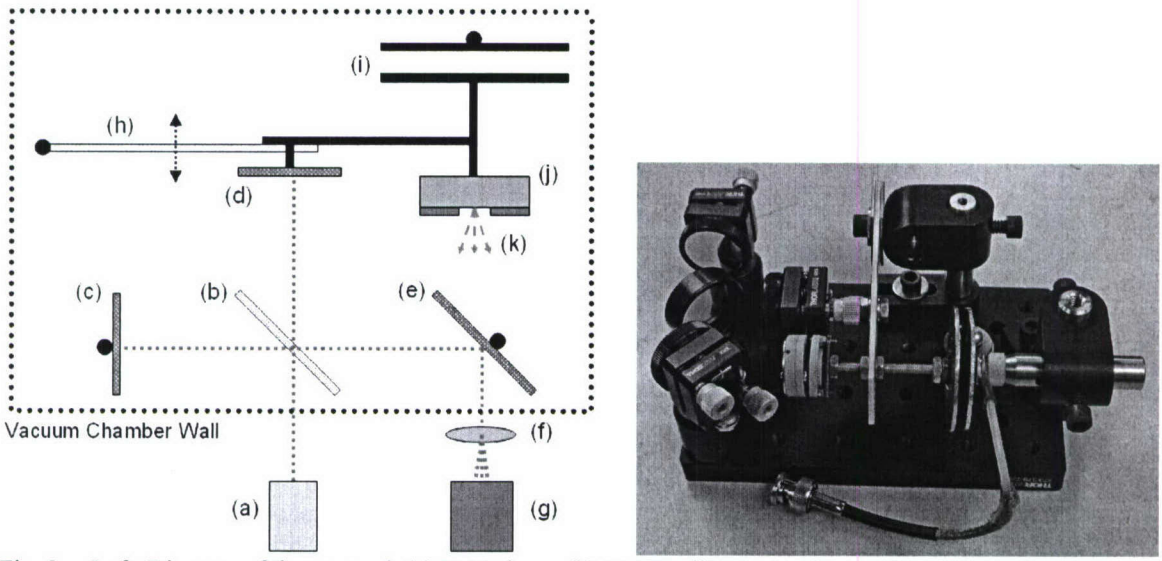

Fig. 8: Left: Diagram of thrust stand, (a) HeNe laser, (b) 50-50 splitter, (c) reference leg mirror, (d) measurement leg mirror, (e) mirror, (f) beam expander, (g) diode detector, (h) pendulum, (i) calibration plates, (j) FEPT, (k) plasma plume. Right: Photograph of thrust stand.

A randomized block experimental design was made with time as the blocking variable. Thruster data was taken alternating with various magnitudes of calibration impulses. Four data points were taken for each of the two FEPT setpoints. The results are shown in Fig. 9. The

experimental data points are the average of four shots and the error bars are the range of data. The calibration line was generated by performing a linear regression on the calibration impulses. The peak arm deflection values found with the FEPT were input to this equation for the calibration line, with the output considered to be the FEPT average thrust.

The mean average thrusts for the two different setpoints were found to be statistically different. With V_{max}=900 V, the average thrust was 68.5 μN with a range of 61-75 μN. With V_{max}=1.0 kV, the average thrust was 74 μN with a range of 68-87 μN. These values are ~30% higher than the calculated thrust of 52 μN. This increased thrust may be attributed to flows of neutral particles or ferroelectric microparticles.

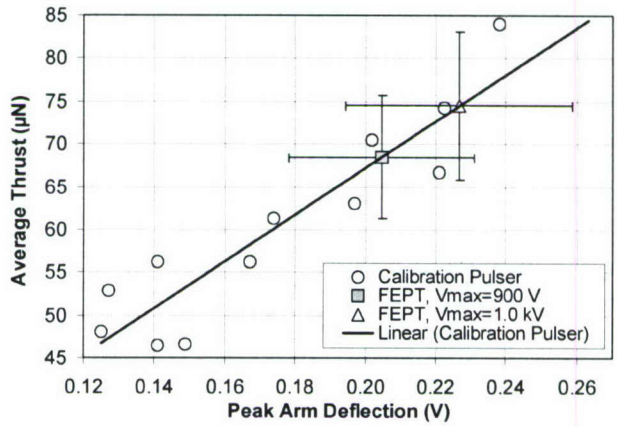

Fig. 9: Measured thrust for two different setpoints.

To measure the mass flow rate of the FEPT, the thruster was weighed before and after operation. The amount of mass change divided by the time of operation is the mass flow rate. As shown, the mass loss per second is calculated to be -26.4 μg/s with a 95% confidence interval of -15.1 to -37.8 μg/s.

The measured thrust range can be combined with the measured mass loss rates to find the values of specific impulse for the thruster. In the previous section, the range in thrust was found to be 68 to 87 μN. With a range of mass flow rates of -15.1 to -37.8 μg/s, the specific impulse range is 183 to 587 s. This impulse is due to both accelerated ions as well as neutrals flowing from the FEPT.

Table II: Summary of microthruster characteristics.

Specific Impulse (measured)	183-587 s
Specific Impulse (ions only)	1350-5300 s
Thrust (measured)	68-87 μN
Thrust (ions only)	17-67 μN
Average Power	4-20 W
Impulse Bit	<1 nN*s
Thrust Efficiency	1.0-4.2 %
Thruster Mass	5.7 g
Estimated Neutral Particle Energy	0.07-15 eV
Mass Loss Rate (ions only)	0.3-5 μg/s
Mass Loss Rate (measured)	15.1 - 37.8 μg/s

6) Summary

One advantage of the FEPT is its compact, low-mass, and low-complexity design. The thruster electrodes, crystal, and mounting hardware have a mass of just 5.7 g. Although for testing we have mainly used large, laboratory rf power supplies, we have also built a low-mass class-E amplifier which has a mass less than 50 g. One proposed scheme for FEPT propellant is to load solid material on the aperture surface. The ablation and acceleration of this material serves as the mass transfer for the thruster. Therefore, there may not be any additional necessary hardware for propellant management. This serves to further reduce the complexity of the thruster.

Another feature of the FEPT is the ability to produce very low impulse bits, where impulse bit is defined as the smallest possible impulse deliverable by the thruster. With an average thrust of ~70 μN and a frequency of operation of around 385 kHz, impulse bits of 70 μN / 385 kHz = 181 pN*s are realizable. However, for certain operating frequencies ion bursts do not start for several cycles after the onset of the applied rf burst. Therefore, a conservative estimate of 1 nN*s is made for the impulse bit.

Table II is a summary of the FEPT characteristics. One characteristic that stands out is the difference between the measured quantities and the quantities assuming the beam is only composed of ions. The hypothesized reason for this is the presence of neutral particles in the beam. This is consistent with the fact that measured specific impulses are smaller than as calculated assuming ions only. The mass expelled from the thruster is 66.9-99.2% neutral particles.

7) Archival publications (published) during reporting period

Dissertation

M.A. Kemp, "The ferroelectric plasma thruster," PhD. Dissertation, Dept. Elect. Comp. Eng., Univ. Missouri-Columbia, May 2008.

Journal Articles

M.A. Kemp and S.D. Kovaleski, "Thrust measurements of the ferroelectric plasma thruster," *IEEE Trans. Plasma Sci.*, April 2008. (accepted)

D. L. Sullivan, M.A. Kemp, and S.D. Kovaleski, "Characterization of a ferroelectric atmospheric pressure plasma source," *IEEE Trans. Plasma Sci.,* vol. 35, no. 5, Oct. 2007.

M.A. Kemp and S.D. Kovaleski, "Piezoelectric resonance effect in a radio frequency driven ferroelectric plasma source," *IEEE Trans. Plasma Sci.*, vol. 35, no. 3, pp. 578-581, Jun. 2007.

M.A. Kemp and S.D. Kovaleski, "Ferroelectric plasma thruster for microspacecraft propulsion," *J. Appl. Phys.,* vol. 100, no. 11, p. 113306, Dec. 2006.

Conference Papers

M.A. Kemp and S.D. Kovaleski, "Thrust and Particle Emission Measurements in a Ferroelectric Plasma Thruster," 43rd AIAA/ASME/SAE/ASEE Joint Propulsion Conference, Jul. 2007. (oral presentation)

M.A. Kemp and S.D. Kovaleski, "Plasma measurements of a radio frequency driven ferroelectric plasma thruster for microspacecraft propulsion," 42nd AIAA/ASME/SAE/ASEE Joint Propulsion Conference, Jul. 2006. (oral presentation)

Conference Presentations

M.A. Kemp and S.D. Kovaleski, "Effect of piezoelectric resonance in a ferroelectric plasma source," Pulsed Power Plasma Science Conference, 2007. (poster presentation)

M.A. Kemp and S.D. Kovaleski, "Optimization of the ferroelectric plasma thruster for microspacecraft propulsion," Pulsed Power Plasma Science Conference, 2007. (invited oral presentation)

D.L. Sullivan, M.A. Kemp, and S.D. Kovaleski, "Characterization of a ferroelectric plasma source operated at atmospheric pressure," Pulsed Power Plasma Science Conference, 2007. (poster presentation)

M.A. Kemp and S.D. Kovaleski, "Plasma and thruster characteristics of a ferroelectric plasma thruster," 48th Meeting of the Division of Plasma Physics, Oct. 2006. (oral presentation)

S.D. Kovaleski, D. Sullivan, and M.A. Kemp, "An RF driven, ferroelectric, atmospheric-pressure plasma source," 48th Meeting of the Division of Plasma Physics, Oct. 2006. (poster presentation)

M.A. Kemp and S.D. Kovaleski, "A study of particle emission from a radio frequency driven ferroelectric plasma thruster," 32nd IEEE International Conference on Plasma Science, Jun. 2006. (poster presentation)